frontiers | Frontiers in Endocrinology

TYPE Original Research
PUBLISHED 15 August 2024
DOI 10.3389/fendo.2024.1403523

Check for updates

OPEN ACCESS

EDITED BY
Sidong Yang,
The University of Queensland, Australia

REVIEWED BY
Joe Kodama,
University of Maryland, United States
Hongfei Xiang,
The Affiliated Hospital of Qingdao University, China

*CORRESPONDENCE
Gang Rui
reigang@163.com
Guang-Xun Lin
linguangxun@hotmail.com

†These authors have contributed equally to this work

RECEIVED 20 March 2024
ACCEPTED 24 July 2024
PUBLISHED 15 August 2024

CITATION
Chen D-Q, Que Z-Q, Xu W-B, Xiao K-Y, Sun N-K, Song H-Y, Feng J-Y, Lin G-X and Rui G (2024) Nucleotide polymorphism-based study utilizes human plasma liposomes to discover potential therapeutic targets for intervertebral disc disease. *Front. Endocrinol.* 15:1403523. doi: 10.3389/fendo.2024.1403523

COPYRIGHT
© 2024 Chen, Que, Xu, Xiao, Sun, Song, Feng, Lin and Rui. This is an open-access article distributed under the terms of the Creative Commons Attribution License (CC BY). The use, distribution or reproduction in other forums is permitted, provided the original author(s) and the copyright owner(s) are credited and that the original publication in this journal is cited, in accordance with accepted academic practice. No use, distribution or reproduction is permitted which does not comply with these terms.

Nucleotide polymorphism-based study utilizes human plasma liposomes to discover potential therapeutic targets for intervertebral disc disease

Ding-Qiang Chen[1,2†], Zhi-Qiang Que[1†], Wen-Bin Xu[1], Ke-Yi Xiao[1,2], Nai-Kun Sun[1], Hong-Yu Song[1], Jin-Yi Feng[1], Guang-Xun Lin[1,2*] and Gang Rui[1,2*]

[1]Department of Orthopedics, The First Affiliated Hospital of Xiamen University, School of Medicine, Xiamen University, Xiamen, Fujian, China, [2]The School of Clinical Medicine, Fujian Medical University, Fuzhou, China

Background: While intervertebral disc degeneration (IVDD) is crucial in numerous spinally related illnesses and is common among the elderly, the complete understanding of its pathogenic mechanisms is still an area of ongoing study. In recent years, it has revealed that liposomes are crucial in the initiation and progression of IVDD. However, their intrinsic mediators and related mechanisms remain unclear. With the development of genomics, an increasing amount of data points to the contribution of genetics in the etiology of disease. Accordingly, this study explored the causality between liposomes and IVDD by Mendelian randomization (MR) analysis and deeply investigated the intermediary roles of undetected metabolites.

Methods: According to MR analysis, 179 liposomes and 1400 metabolites were evaluated for their causal association with IVDD. Single nucleotide polymorphisms (SNPs) are strongly associated with the concentrations of liposomes and metabolites. Consequently, they were employed as instrumental variables (IVs) to deduce if they constituted risk elements or protective elements for IVDD. Furthermore, mediation analysis was conducted to pinpoint possible metabolic mediators that link liposomes to IVDD. The inverse variance weighting (IVW) was the main analytical technique. Various confidence tests in the causality estimates were performed, including consistency, heterogeneity, pleiotropy, and sensitivity analyses. Inverse MR analysis was also utilized to estimate potential reverse causality.

Results: MR analysis identified 13 liposomes and 79 metabolites markedly relevant to IVDD. Moreover, the mediation analysis was carried out by choosing the liposome, specifically the triacylglycerol (48:2) levels, which were found to be most notably associated with an increased risk of IVDD. In all, three metabolite-associated mediators were identified (3-methylcytidine levels, inosine 5′-monophosphate (IMP) to phosphate ratio, and adenosine 5′-diphosphate (ADP) to glycine ratio).

Conclusion: The analysis's findings suggested possible causal connections between liposomes, metabolites, and IVDD, which could act as both forecast and prognosis clinical indicators, thereby aiding in the exploration of the pathogenesis behind IVDD.

KEYWORDS

intervertebral disk degeneration, causality, liposome, metabolite, Mendelian randomization

Introduction

Lipid metabolism represents a complicated process for maintaining the body's regular physiological functions. Disorders of lipid metabolism are linked to various human disorders, including cardiovascular and bone diseases (1). IVDD represents a degenerative condition that is notably widespread. As the proteoglycan and water within the nucleus pulposus (NP) gradually decrease, the intervertebral discs (IVD) between the vertebrae may rupture. Subsequently, the herniation of the NP exerts pressure on the spinal nerves, leading to a significant deterioration in the patient's quality of life (2). Furthermore, IVDD is a primary contributor to numerous spine-related conditions, including spinal stenosis and chronic sciatica (3). As the global population ages rapidly, the prevalence of IVDD continues to be high, posing a significant challenge to both public health and socioeconomic development. Nevertheless, existing non-surgical therapies and surgical procedures alike have been found ineffective in reversing the condition of IVDD (4).

Lipid metabolism performs a crucial function in maintaining IVD stability. When lipid metabolic homeostasis is disturbed, the IVD microenvironment is impacted. Disorders of lipid metabolism are strongly associated with the development of IVDD (5). A retrospective clinical study involving 302 hospitalized patients demonstrated that age, high-density lipoprotein cholesterol (HDL-C), and triglycerides (TGs) can influence degeneration levels of patients with symptomatic degenerative lumbar spine without underlying disease (6). Another case-control study with 396 patients and 394 controls showed that abnormal blood lipids may be linked to higher risk of lumbar disc herniation (7). The excess mechanic load on the lumbar spine caused by excess weight due to disorders of lipid metabolism is a logical pathogenic explanation for IVDD (8). However, the presumption of obesity being associated with pain and degenerative disease as a result of joint overload contradicts the fact that non-weight-bearing joints present with similar degenerative disease and related pain (9). An annulus fibrosus (AF) with structural deterioration is intimately linked to IVDD. Unusual mechanical stress is a major factor in annulus fibrosus cell (AFC) apoptosis, which harms the AF structurally and aggravates IVDD (10), and the majority of scholars agree that obesity is a mechanical risk factor for IVDD (11, 12). Nonetheless, the literature indicates that there has been disagreement on its function (13–15). It is not possible to attribute these observed disparities to the mechanical consequences of obesity alone. Obesity has not just mechanical impacts but also metabolic and inflammatory ones (16, 17). It is now acknowledged that adipose tissue is an active organ with a variety of metabolic and inflammatory characteristics. Adipokines, which function both locally and across the body's circulation to reach distant regions and exert pro- or anti-inflammatory effects, are distinct and specialized proteins secreted by adipocytes (18). Obese adipose tissue produces systemic pro-inflammatory substances at a low level over an extended period of time, indicating that obesity-related chronic low-grade inflammation may play a significant role in IVDD. Thus, mechanistically, purely mechanical loading cannot explain the association between obesity and IVDD.

Other possible mechanisms beyond the impact of mechanical strain on the development of IVDD need further investigation. Plasma lipids are typically measured by HDL-C, low-density lipoprotein cholesterol, TGs, and total cholesterol (TC); however, the versatility and range of circulating lipids have been much more understood because to the development of contemporary high-performance lipidomic methods. Lipid classes are more finely delineated and may improve risk assessment for IVDD compared with standard lipids (19). Ultimately, an improved knowledge of the biology of lipid metabolism and its link to the pathogenesis of IVDD could also lead to novel therapeutic options for IVDD.

Presently, the most convincing explanation for the relationship between elevated body fat and IVDD is the internal secretory function of fatty tissue. Obesity increases the impaired cellular metabolism of free fatty acids, which promotes the development of IVDD (1). As a competitive inhibitor of arachidonic acid (AA), eicosapentaenoic acid (EPA) reduces inflammation by preventing the synthesis of lipoxygenase (LOX) and cyclooxygenase (CYC). In an alternative dietary control study, Napier et al. discovered that omega-3 fatty acids (n-3 FA) dietary supplementation lowers systemic inflammation and may even prevent the advancement of degenerative disc degeneration by lowering serum AA/EPA ratios. This was observed in a mice model of acupuncture-elicited IVDD (20). However, further exploration is needed to identify other possible metabolic factors linking liposomes to IVDD. The majority of existing research in this area

has not conclusively established whether the liposomes examined have a direct causal connection to IVDD. Therefore, the search for IVDD-causing liposomes and the metabolite mediators that play an essential role between them could contribute to the mechanistic study of IVDD and it aids in making clinical judgments prior to the development of serious spinal conditions.

Luckily, the increasing attention on IVDD in the elderly population, genome-wide association study (GWAS) data related to IVDD has been concluded, uncovering genetic insights linked to the condition. Therefore, the possible causative relationship between liposomes, metabolites, and IVDD was assessed using MR techniques. A two-step MR approach was also used to identify possible metabolic mediators between liposomes and IVDD. As gametogenesis adheres to Mendel's principles of inheritance, the distribution of parental genes to offspring occurs randomly in accordance with Mendelian genetics. Consequently, genetic types might not correlate with elements that affect the accuracy of observational research. MR techniques are capable of differentiating diseases from their underlying causes, thereby preventing the misinterpretation of causal relationships (21). Consequently, employing genetic variants associated with the target characteristic as IVs, MR emerges as a highly dependable analyzing technique that shows promise in determining exposure-outcome causality, eliminating confounding variables, measuring inaccuracies and correcting causal misinterpretations (22–24). Furthermore, genetic variation must be extracted from exposure- and outcome-related information in order to use two-sample MR designs, which enhances the statistical strength in confirming causal relationships between exposures and outcomes (25, 26).

Materials and methods

Study design

This research utilized the TwosampleMR software package. SNPs act as genetic proxies for inferring the influence of exposures on outcomes. Three presumptions should be met by genetic tools in MR analysis: SNPs are linked to the exposures, they are not connected with confounding factors that could interfere with the causality between the exposures and the outcomes, and their relationship with the outcomes are mediated exclusively through the exposures.

Data sources

Summary statistics for liposomes (covering 4 major lipid categories: glycerolipids, glycerophospholipids, sphingolipids, and sterols) were obtained from a large-scale GWAS study by Linda Ottensmann and his team, which performed univariate and multivariate genome-wide analyses of 179 lipids from 7174 Finnish individuals. The GWAS catalog database provides access to the data for download (accession codes GCST90277238-GCST90277416) (19). Summary statistics for metabolites were obtained from a series of large GWASs study by Yiheng Chen and his team, which included 1091 metabolites and 309 metabolite ratios across 8299 participants. The GWAS catalog database provides access to the data for download (accession numbers from GCST90199621-90201020) (27). IVDD-related GWAS data from 184,683 subjects from European populations, including 20,001 IVDD cases and 164,682 controls, were sourced from the FinnGen repository, which contained a total of 16,380,337 SNPs.

The process of selecting instrumental variables involved

SNPs were incorporated based on achieving a threshold of genome-wide significance ($P < 1 \times 10^{-5}$). For the inverse MR analysis, the IV significance threshold for IVDD was defined as 5×10^{-8}. To avoid strong linkage disequilibrium (LD), an LD threshold of $r^2 < 0.001$ was established. Additionally, the selection was limited to SNPs with an F-value greater than 10 to minimize the risk of weak instrumental bias. (Supplementary Tables 1, 2; Table 1).

Data analysis

Utilizing the IVW method can provide a reliable assessment of causal relationships between exposures and outcomes, provided that each genetic variant meets the instrumental variable criteria (28). The Egger and weighted median methods can yield trustworthy causal inferences for a range of genetic variants, utilizing pooled data and operating under more lenient conditions. Even if up to 50 percent the data comes from genetic variants that are null IVs, the weighted median estimation continues to deliver coherent causality assessments (29). Additionally, MR-Egger regression and the MR-pleiotropy residual sum and outlier methods were used to detect and correct for pleiotropy. MR-Egger regression techniques aggregate causal effect estimates from multiple individual variables to assess and adjust for potential pleiotropy imbalances (30). Weighted linear regression of genetic outcome data to genetic exposure data was the approach that MR-Egger used. The causal estimation is represented by the slope of the linear regression, while the interception reflects the average impact of multiplicative effects from genetic variations (31). The heterogeneity among SNP estimates was evaluated using the statistical measure known as Cochran's Q (32). A *P*-value greater than 0.05 suggests that neither horizontal pleiotropy nor heterogeneity is present. Ultimately, a leave-one-out approach was applied to the sequential removal of each SNP in order to verify that none of the SNPs had a significant effect on the outcome.

Primary analysis

First, to determine the causality between liposomes and IVDD or metabolites and IVDD (Figure 1), two-sample MR analyses were used. The primary analytical technique employed was the IVW technique. Additionally, validation was conducted using MR Egger, weighted median, simple mode, and weighted mode methods (33).

10.3389/fendo.2024.1403523

TABLE 1 Characteristics of significant SNPs for intervertebral disk degeneration on liposomes.

SNP	pval.exposure	chr.exposure	pos.exposure	samplesize.exposure	beta.exposure	se.exposure	id.exposure	effect_allele.exposure	other_allele.exposure	eaf.exposure	exposure	R2	F
rs12308843	4.36E-08	12	23974404	184683	0.0689	0.0126	finn-b-M13_INTERVERTEB	C	G	0.3103	intervertebral disk degeneration	0.002031938	376.0243903
rs3010043	4.73E-09	1	183942175	184683	-0.0836	0.0143	finn-b-M13_INTERVERTEB	G	A	0.7913	intervertebral disk degeneration	0.002308374	427.2991764
rs3135840	9.27E-10	4	1796539	184683	-0.0816	0.0133	finn-b-M13_INTERVERTEB	T	A	0.2631	intervertebral disk degeneration	0.002581902	478.062514
rs4148946	3.00E-08	10	73770073	184683	0.0647	0.0117	finn-b-M13_INTERVERTEB	T	C	0.554	intervertebral disk degeneration	0.002068632	382.8289073
rs4473430	2.42E-08	2	69582895	184683	-0.0651	0.0117	finn-b-M13_INTERVERTEB	T	C	0.5523	intervertebral disk degeneration	0.002095821	387.8711576
rs62099230	3.27E-11	18	50721712	184683	0.0785	0.0118	finn-b-M13_INTERVERTEB	A	G	0.404	intervertebral disk degeneration	0.002967542	549.6798979
rs6470763	6.82E-09	8	130720646	184683	-0.092	0.0159	finn-b-M13_INTERVERTEB	C	G	0.1652	intervertebral disk degeneration	0.002334523	432.1508852

chr, chromosome; pos, position; beta, effect estimate; se, standard error of beta; eaf, effect allele frequency; R2, explained phenotypic variability; F, F statistic; F = R2 (N − K − 1)/(K (1 − R2)); K, number of SNPs; N, sample size; R2, explained phenotypic variability.

Mediation analysis

Mediation analysis represents a novel technique for ascertaining if a variable mediates between two variables, which enables the construction of pathways from exposure factors to outcomes through mediators, aiding in the elucidation of the mechanisms through which exposure factors affect outcomes (34). For instance, both liposomes and metabolites have a significant causal impact on IVDD, with the liposome additionally having a significant causal effect on the metabolites. This setup establishes a triangular interaction where liposomes act as the exposure, metabolites serve as the mediator, and IVDD represents the outcome. The subsequent equation was applied: Mediation ratio = c × d/a. The total influence of liposomes on IVDD is dissected into two components: the immediate effect of liposomes on IVDD and the indirect influence mediated by the metabolites. The subsequent steps determine the percentage of mediating effect: initially, the impact of liposomes on metabolites is calculated to derive the value 'c'; the next step involves computing the influence of metabolites on IVDD to ascertain the value 'd'. The mediation impact percentage is subsequently determined by division of the indirect impact (c × d) by the total impact of liposomes on IVDD (a). (Figure 1). A larger percent of mediating impacts suggests that a greater portion of liposome impacts on IVDD are mediated through metabolites.

Statistical analysis

This study was executed using R version 4.3.1. The "Forestploter" package was leveraged to create forest plots. Additionally, the "MRPRESSO" package was used for detecting outlier.

Results

MR analysis results of liposomes and IVDD

MR analysis showed a total of 13 liposomes were identified as significantly associated with IVDD, of which seven liposomes were risk factors, including diacylglycerol (18:1_18:3) levels, phosphatidylcholine (16:0_18:3) levels, and triacylglycerol (48:2) levels, etc. And six liposomes as protective factors, including phosphatidylcholine (14:0_16:0) levels, phosphatidylcholine (16:0_20:4) levels, sphingomyelin (d36:2) levels, etc (Table 2). Reverse MR analysis revealed a significant link between IVDD and one liposome phosphatidylcholine (O-16:0_20:3) levels (Table 3).

MR analysis results of metabolite and IVDD

In the two-sample MR analysis, a total of 79 metabolites were found to be significantly linked to IVDD. Among these, 40 were identified as risk factors, such as N6-carbamoylthreonyladenosine levels, 2-hydroxy-3-methylvalerate levels, N-methyltaurine levels,

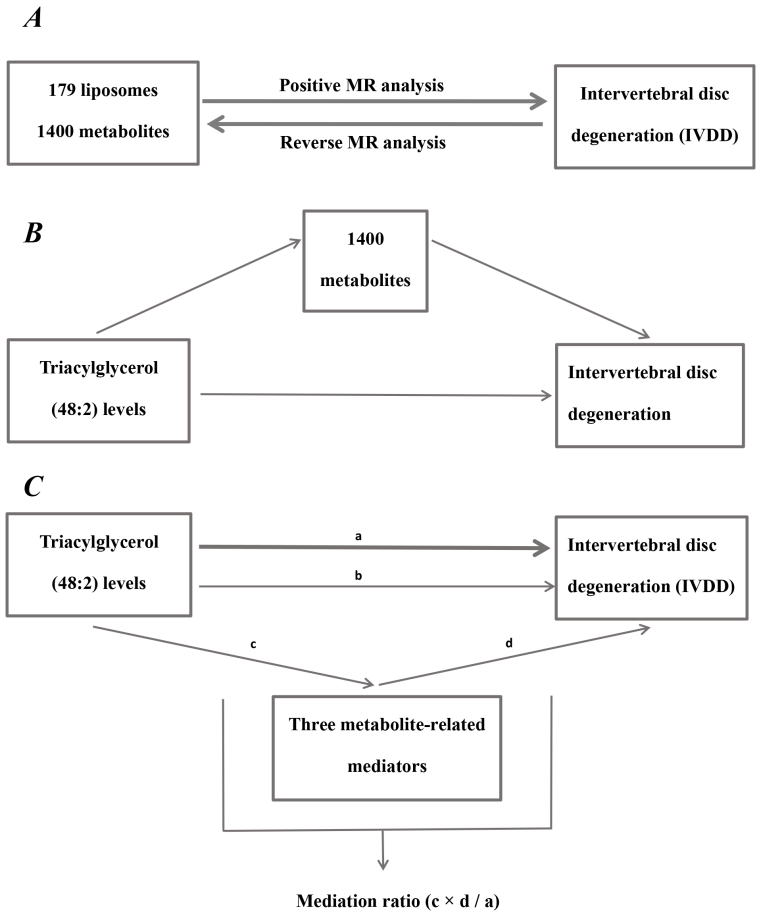

FIGURE 1
Diagram of analytical relationships. **(A)** Diagram of positive and reverse MR analysis between 179 liposomes and 1400 metabolites with IVDD. **(B)** Diagram of mediated MR analysis. Triacylglycerol (48:2) levels as the exposure factor, 1400 metabolites as mediators, and IVDD as the outcome. **(C)** Diagram of mediation ratio calculation. 'a' indicates the total influence of triacylglycerol (48:2) levels on IVDD. 'c' indicates the effect of triacylglycerol (48:2) levels on three metabolite-related mediators. 'd' indicates the effect of three metabolite-related mediators on IVDD. 'b' indicates direct effects = a - c × d (indirect impact). Mediation ratio = c × d/a.

2-hydroxydecanoate levels, etc. Conversely, the remaining 39 metabolites were recognized as protective factors, including glucose to mannitol to sorbitol ratio, proline to trans-4-hydroxyproline ratio, mannose to mannitol to sorbitol ratio, etc (Supplementary Table 3).

Findings from the mediation MR analysis

To explore how liposomes might be involved in the development of IVDD, we conducted a mediation analysis using MR, with metabolites serving as the mediating factors between liposomes and IVDD. Three distinct mediating associations were discovered. Triacylglycerol (48:2) levels influence IVDD risk via the three metabolites, with the mediation via the ADP to glycine ratio being consistent with the overall effect, with a mediating effect percentage of 7.13%. In contrast, the mediating effects of 3-methylcytidine levels and IMP to phosphate ratio were opposite to the overall impact (Figure 2).

Sensitivity analysis

Sensitivity analyses revealed some MR findings were heterogeneous (Tables 4, 5; Supplementary Table 4). The heterogeneity arises from the intrinsic nature of MR (35). When a gene is located on the same chromosome, it exhibits correlation without adhering to patterns of genetic independence in variation. Furthermore, IVs derived from various unit of analysis, studies, populations, etc., are probably displaying heterogeneity, which can impact the outcomes of MR analyses. The pleiotropy assessment disclosed instances of horizontal pleiotropy among certain liposomes and metabolites in relation to IVDD analysis (Tables 4, 5; Supplementary Table 4). This suggests that segments of the IVs influence the outcomes through additional factors. However, the existing methodologies do not facilitate a comprehensive examination of the specific traits of every SNP. Consequently, we incorporated only those liposomes and metabolites that cleared the pleiotropy test in the following intermediary analysis (Table 6). Thus, the findings of this study maintain a high level of credibility.

TABLE 2 Causal effects of liposomes on intervertebral disk degeneration.

Exposure	Outcome	Method	NSNPs	Pval	b	lo_ci	up_ci	OR	OR_lci95	OR_uci95
Sterol ester (27:1/22:6) levels	Intervertebral Disk Degeneration	MR Egger	23	0.449785537	-0.047918711	-0.169869035	0.074031613	0.953211269	0.843775314	1.076840847
		Weighted median	23	0.071462172	-0.068663623	-0.143325767	0.005998521	0.933640683	0.866471755	1.006016548
		Inverse variance weighted	23	0.024567029	-0.059510025	-0.111392674	-0.007627376	0.942226087	0.894587399	0.992401638
		Simple mode	23	0.788714782	0.020895484	-0.130081778	0.171872746	1.021115323	0.878023625	1.187526706
		Weighted mode	23	0.784909072	0.014280159	-0.087025546	0.115585865	1.014382608	0.916653678	1.122530897
Diacylglycerol (18:1_18:3) levels	Intervertebral Disk Degeneration	MR Egger	22	0.841075681	0.015365138	-0.132883402	0.163613678	1.015483789	0.875567176	1.177759233
		Weighted median	22	0.07857165	0.074216924	-0.008479107	0.156912954	1.077040416	0.991556739	1.169893775
		Inverse variance weighted	22	0.02743991	0.065194312	0.007249126	0.123139498	1.067366406	1.007275464	1.131042188
		Simple mode	22	0.185807059	0.110986349	-0.048041891	0.270014588	1.117379653	0.95309386	1.309983561
		Weighted mode	22	0.223858178	0.092987508	-0.052428617	0.238403633	1.097448026	0.948922055	1.26922139
Phosphatidylcholine (14:0_16:0) levels	Intervertebral Disk Degeneration	MR Egger	19	0.344911244	0.072019423	-0.073276873	0.217315718	1.074676217	0.929343484	1.242736395
		Weighted median	19	0.15065017	-0.063622919	-0.150387154	0.023141317	0.93835877	0.860374814	1.023411155
		Inverse variance weighted	19	0.0413156	-0.066602776	-0.130582739	-0.002622812	0.935566757	0.877583879	0.997380624
		Simple mode	19	0.434014701	-0.06381949	-0.220133006	0.092494026	0.938174334	0.802412065	1.096906588
		Weighted mode	19	0.469025493	-0.060081911	-0.219284219	0.099120396	0.941687396	0.803093431	1.104199233
Phosphatidylcholine (16:0_18:3) levels	Intervertebral Disk Degeneration	MR Egger	23	0.65448655	-0.034564452	-0.183785626	0.114656721	0.966026075	0.832114169	1.121488388
		Weighted median	23	0.102787931	0.074942969	-0.015090455	0.164976392	1.077822679	0.985022836	1.179365276
		Inverse variance weighted	23	0.044439415	0.064585868	0.001604179	0.127567557	1.066717171	1.001605466	1.136061614

(Continued)

10.3389/fendo.2024.1403523

TABLE 2 Continued

Exposure	Outcome	Method	NSNPs	Pval	b	lo_ci	up_ci	OR	OR_lci95	OR_uci95
		Simple mode	23	0.429240879	0.084285661	-0.120844348	0.28941567	1.087939631	0.886171883	1.335646802
		Weighted mode	23	0.325429004	0.095755788	-0.090836201	0.282347778	1.100490279	0.913167274	1.326239877
Phosphatidylcholine (16:0_20:4) levels	Intervertebral Disk Degeneration	MR Egger	24	0.13013339	-0.03852322	-0.086542936	0.009496497	0.962209362	0.917096172	1.009541732
		Weighted median	24	0.076560629	-0.033951334	-0.071525924	0.003623256	0.966618545	0.930972143	1.003629828
		Inverse variance weighted	24	0.045960097	-0.032517712	-0.064452779	-0.000582645	0.968005304	0.937580386	0.999417524
		Simple mode	24	0.42878099	-0.043796607	-0.150365709	0.062772495	0.957148615	0.860393265	1.064784568
		Weighted mode	24	0.098841262	-0.034922513	-0.074715321	0.004870294	0.965680241	0.928007633	1.004882173
Phosphatidylcholine (O-16:0_20:3) levels	Intervertebral Disk Degeneration	MR Egger	16	0.006126584	0.225248738	0.088292339	0.362205136	1.252634255	1.0923074	1.436493588
		Weighted median	16	0.071959018	0.078474876	-0.007005116	0.163954867	1.081636179	0.993019363	1.17816114
		Inverse variance weighted	16	0.00554003	0.085475558	0.025078208	0.145872908	1.089234938	1.025395312	1.157049127
		Simple mode	16	0.906793308	-0.008657073	-0.151150174	0.133836028	0.991380292	0.859718581	1.143205351
		Weighted mode	16	0.061309412	0.113119275	0.003505734	0.222732816	1.119765485	1.003511886	1.249486686
Sphingomyelin (d36:2) levels	Intervertebral Disk Degeneration	MR Egger	24	0.338868311	-0.060504388	-0.181801968	0.060793193	0.941289639	0.833766436	1.062679122
		Weighted median	24	0.140066187	-0.056237842	-0.130939867	0.018464184	0.945314274	0.877270526	1.018635701
		Inverse variance weighted	24	0.000287281	-0.096690669	-0.148948581	-0.044432756	0.907836785	0.861613417	0.95653992
		Simple mode	24	0.626967934	-0.032987251	-0.164240952	0.098266449	0.967550894	0.84853754	1.103256708
		Weighted mode	24	0.393496455	-0.042730452	-0.139039483	0.05357858	0.958169628	0.87019367	1.055039894
Sphingomyelin (d38:2) levels	Intervertebral Disk Degeneration	MR Egger	31	0.31898261	-0.051546411	-0.151185413	0.048092592	0.94975957	0.859688286	1.049267804
		Weighted median	31	0.421373415	-0.025968804	-0.089272628	0.037335019	0.974365485	0.914596195	1.038040726

(Continued)

10.3389/fendo.2024.1403523

TABLE 2 Continued

Exposure	Outcome	Method	NSNPs	Pval	b	lo_ci	up_ci	OR	OR_lci95	OR_uci95
		Inverse variance weighted	31	0.019611113	-0.055288302	-0.101723056	-0.008853548	0.946212314	0.903279675	0.99118553
		Simple mode	31	0.478609316	-0.046957	-0.175227897	0.081313897	0.954128424	0.839265733	1.084711331
		Weighted mode	31	0.631878214	-0.019380057	-0.097856153	0.059096038	0.980806529	0.906779332	1.060877121
Sphingomyelin (d42:2) levels	Intervertebral Disk Degeneration	MR Egger	38	0.848554686	-0.00869274	-0.097273015	0.079887535	0.991344933	0.907308264	1.083165243
		Weighted median	38	0.46398265	-0.023707876	-0.087161573	0.039745821	0.976570948	0.916528997	1.040546256
		Inverse variance weighted	38	0.041817716	-0.048205232	-0.09462634	-0.001784125	0.952938193	0.909712794	0.998217466
		Simple mode	38	0.526932209	0.050081762	-0.103598308	0.203761833	1.051357054	0.901587385	1.226006124
		Weighted mode	38	0.29159126	0.055920661	-0.046522323	0.158363646	1.057513779	0.954543252	1.171592162
Triacylglycerol (48:2) levels	Intervertebral Disk Degeneration	MR Egger	24	0.106048361	0.120252422	-0.019593905	0.26009875	1.127781493	0.980596808	1.297058165
		Weighted median	24	0.045882351	0.0847036	0.001547469	0.16785973	1.088394418	1.001548667	1.182770692
		Inverse variance weighted	24	0.006114398	0.079909912	0.022781075	0.137038749	1.083189481	1.023042546	1.146872587
		Simple mode	24	0.405868326	0.062287543	-0.081894357	0.206469443	1.064268323	0.92136929	1.229330168
		Weighted mode	24	0.259820507	0.07639007	-0.05320548	0.20598562	1.079383527	0.94818516	1.228735535
Triacylglycerol (49:1) levels	Intervertebral Disk Degeneration	MR Egger	25	0.609562849	0.035242725	-0.098167124	0.168652574	1.03587111	0.906497394	1.183708816
		Weighted median	25	0.022337169	0.089314087	0.012689403	0.165938772	1.093424033	1.012770255	1.18050082
		Inverse variance weighted	25	0.031312709	0.063876476	0.005728089	0.122024862	1.065960719	1.005744526	1.12978219
		Simple mode	25	0.161696862	0.120719681	-0.043150023	0.284589386	1.128308582	0.957767692	1.329216121
		Weighted mode	25	0.149027885	0.115098697	-0.036219891	0.266417284	1.121984168	0.964428201	1.305279617

(Continued)

10.3389/fendo.2024.1403523

TABLE 2 Continued

Exposure	Outcome	Method	NSNPs	Pval	b	lo_ci	up_ci	OR	OR_lci95	OR_uci95
Triacylglycerol (49:2) levels	Intervertebral Disk Degeneration	MR Egger	17	0.784613378	-0.020314298	-0.163404604	0.122776009	0.979890647	0.84924751	1.130631141
		Weighted median	17	0.122390038	0.068273563	-0.018348999	0.154896125	1.070658161	0.981818319	1.167536677
		Inverse variance weighted	17	0.032730104	0.06816972	0.005598775	0.130740664	1.070546986	1.005614478	1.139672185
		Simple mode	17	0.746137719	-0.027341979	-0.190040274	0.135356317	0.973028429	0.826925829	1.144944674
		Weighted mode	17	0.422051473	0.068284207	-0.09413872	0.230707134	1.070669557	0.910156496	1.259490323
Triacylglycerol (54:3) levels	Intervertebral Disk Degeneration	MR Egger	30	0.81516397	-0.014103229	-0.131240462	0.103034004	0.985995756	0.877006862	1.108529103
		Weighted median	30	0.237056075	0.042949496	-0.028246916	0.114145909	1.043885174	0.972148298	1.120915664
		Inverse variance weighted	30	0.006716964	0.06432523	0.017811802	0.110838659	1.066439181	1.017971378	1.117214639
		Simple mode	30	0.309226505	0.06141828	-0.054891589	0.177728149	1.063343596	0.946587763	1.194500551
		Weighted mode	30	0.296679268	0.048860784	-0.041254413	0.138975981	1.050074153	0.959584968	1.1490965

SNP, single nucleotide polymorphism; b, beta; OR, odds ratio; ci, confidence interval.

10.3389/fendo.2024.1403523

TABLE 3 Causal effects of intervertebral disk degeneration on liposomes.

Exposure	Outcome	Method	NSNPs	Pval	b	lo_ci	up_ci	OR	OR_lci95	OR_uci95
Intervertebral Disk Degeneration	Sterol ester (27:1/22:6) levels	MR Egger	7	0.75438629	0.355622052	-1.753045973	2.464290076	1.427068088	0.173245438	11.75513394
		Weighted median	7	0.56848866	0.076991805	-0.187622545	0.341606154	1.080033225	0.828927531	1.407205967
		Inverse variance weighted	7	0.76532834	0.035977287	-0.2002625	0.272217074	1.036632301	0.818515865	1.31287196
		Simple mode	7	0.319436811	0.222054462	-0.178945882	0.623054807	1.24863938	0.836151149	1.864615391
		Weighted mode	7	0.316598113	0.222054462	-0.176386877	0.620495801	1.24863938	0.838293604	1.85984993
Intervertebral Disk Degeneration	Diacylglycerol (18:1_18:3) levels	MR Egger	7	0.887155052	-0.119014374	-1.681468291	1.443439543	0.887795039	0.186100526	4.235238077
		Weighted median	7	0.815735958	-0.027831732	-0.261919814	0.20625635	0.972552002	0.76957273	1.229068235
		Inverse variance weighted	7	0.893042084	-0.01304125	-0.203147084	0.177064583	0.987043418	0.816158189	1.193708184
		Simple mode	7	0.692219217	-0.068799095	-0.393331046	0.255732856	0.933514209	0.674805319	1.29140769
		Weighted mode	7	0.693054774	-0.065876632	-0.377526972	0.245773709	0.93624636	0.68555471	1.278610202
Intervertebral Disk Degeneration	Phosphatidylcholine (14:0_16:0) levels	MR Egger	7	0.953785586	-0.053070149	-1.760609158	1.65446886	0.948313487	0.171940093	5.230301161
		Weighted median	7	0.889735629	-0.018726564	-0.283472664	0.246019536	0.981447689	0.75316371	1.278924559
		Inverse variance weighted	7	0.73125669	0.036398508	-0.171317826	0.244114841	1.037069044	0.842553745	1.276490916
		Simple mode	7	0.869726294	-0.035166857	-0.43787822	0.367544507	0.965444312	0.645404375	1.444184073
		Weighted mode	7	0.869027016	-0.035166857	-0.435703444	0.365369731	0.965444312	0.646809512	1.44104671
Intervertebral Disk Degeneration	Phosphatidylcholine (16:0_18:3) levels	MR Egger	7	0.953824162	-0.046426814	-1.541465417	1.44861179	0.954634424	0.214067174	4.257200524
		Weighted median	7	0.996580474	-0.000511994	-0.23466184	0.233637851	0.999488137	0.790838235	1.263186948
		Inverse variance weighted	7	0.593209475	0.049549041	-0.132251366	0.231349448	1.050797123	0.87612074	1.260299572
		Simple mode	7	0.973655695	-0.006133805	-0.35537456	0.343106949	0.993884968	0.700910861	1.409319479
		Weighted mode	7	0.950277199	-0.011403369	-0.355200793	0.332394054	0.988661403	0.701032667	1.39430217
Intervertebral Disk Degeneration	Phosphatidylcholine (16:0_20:4) levels	MR Egger	7	0.406708715	-0.687933907	-2.176974247	0.801106432	0.502613443	0.113384084	2.228004701
		Weighted median	7	0.941411815	0.008830679	-0.226668463	0.24432982	1.008869784	0.797185035	1.276765364
		Inverse variance weighted	7	0.745134751	-0.03004461	-0.211202605	0.151113385	0.970402243	0.809610019	1.163128532
		Simple mode	7	0.962231631	-0.009070613	-0.369221441	0.351080215	0.990970401	0.691272317	1.420601275
		Weighted mode	7	0.906443483	-0.020264974	-0.344296522	0.303766575	0.979938981	0.708718746	1.35495274
Intervertebral Disk Degeneration	Phosphatidylcholine (O-16:0_20:3) levels	MR Egger	7	0.153366002	1.35436911	-0.2237098	2.932448019	3.874315917	0.79954713	18.77353225
		Weighted median	7	0.748005822	0.045218361	-0.230649287	0.321086008	1.046256296	0.79401789	1.378624148

(Continued)

10.3389/fendo.2024.1403523

TABLE 3 Continued

Exposure	Outcome	Method	NSNPs	Pval	b	lo_ci	up_ci	OR	OR_lci95	OR_uci95
		Inverse variance weighted	7	0.042354549	0.215020491	0.007416502	0.42262448	1.239887304	1.007444073	1.52596116
		Simple mode	7	0.999294973	0.000179233	-0.381232534	0.381591	1.000179249	0.683019046	1.464612936
		Weighted mode	7	0.991765442	-0.002245968	-0.411445643	0.406953706	0.997756552	0.662691542	1.50223456
Intervertebral Disk Degeneration	Sphingomyelin (d36:2) levels	MR Egger	7	0.395389668	0.708347613	-0.78565092	2.202346147	2.030633094	0.455822901	9.046212364
		Weighted median	7	0.092434121	0.204651166	-0.03372611	0.443028442	1.227096938	0.966836276	1.55741663
		Inverse variance weighted	7	0.113990887	0.146529479	-0.035182999	0.328241956	1.157809061	0.965428728	1.388524894
		Simple mode	7	0.27913175	0.209714989	-0.135808459	0.555238437	1.233326498	0.873009833	1.742356378
		Weighted mode	7	0.251474938	0.209714989	-0.114217665	0.533647643	1.233326498	0.892063764	1.705140723
Intervertebral Disk Degeneration	Sphingomyelin (d38:2) levels	MR Egger	7	0.340895984	0.974630734	-0.840951431	2.790212898	2.650188405	0.431299976	16.28448637
		Weighted median	7	0.114701105	0.197206362	-0.047830978	0.442243703	1.217995363	0.953294901	1.556194943
		Inverse variance weighted	7	0.180869483	0.148357295	-0.068953862	0.365668452	1.159927258	0.933369742	1.441477245
		Simple mode	7	0.215833268	0.272555302	-0.113618823	0.658729428	1.313316086	0.892598129	1.932335602
		Weighted mode	7	0.184589165	0.257195459	-0.07914847	0.593539387	1.293297888	0.923902743	1.810384742
Intervertebral Disk Degeneration	Sphingomyelin (d42:2) levels	MR Egger	7	0.112912504	1.609408246	-0.033433791	3.252250284	4.999851672	0.967118941	25.84844084
		Weighted median	7	0.23322856	-0.165188771	-0.436788896	0.106411355	0.847733662	0.646107813	1.112279324
		Inverse variance weighted	7	0.860540251	0.021496652	-0.218325076	0.261318379	1.021729369	0.803864082	1.29864106
		Simple mode	7	0.364609067	-0.212175094	-0.636217471	0.211867284	0.808823065	0.5292907	1.235983839
		Weighted mode	7	0.327264034	-0.202838929	-0.575650913	0.169973056	0.816409731	0.562338716	1.185272915
Intervertebral Disk Degeneration	Triacylglycerol (48:2) levels	MR Egger	7	0.871152648	0.132207745	-1.385823392	1.650238883	1.141345404	0.25011777	5.208223835
		Weighted median	7	0.285134056	-0.138528874	-0.392554027	0.115496279	0.870638112	0.675329859	1.122430338
		Inverse variance weighted	7	0.246904614	-0.108194471	-0.29133728	0.074948338	0.897453051	0.747263598	1.077828467
		Simple mode	7	0.329468803	-0.213719568	-0.60848183	0.181042694	0.807574823	0.544176395	1.198466346
		Weighted mode	7	0.32222399	-0.210902956	-0.594164483	0.172358572	0.809852655	0.552023599	1.188103777
Intervertebral Disk Degeneration	Triacylglycerol (49:1) levels	MR Egger	7	0.876784406	-0.202256275	-2.631956172	2.227443622	0.816885554	0.071937602	9.276122472
		Weighted median	7	0.131633512	-0.229029429	-0.526767854	0.068708996	0.795305128	0.590510505	1.071124462
		Inverse variance weighted	7	0.11680968	-0.215895238	-0.485711588	0.053921113	0.805819717	0.61525923	1.055401341
		Simple mode	7	0.785095877	-0.067908711	-0.534638264	0.398820842	0.934345765	0.585881186	1.490066638

(Continued)

10.3389/fendo.2024.1403523

TABLE 3 Continued

Exposure	Outcome	Method	NSNPs	Pval	b	lo_ci	up_ci	OR	OR_lci95	OR_uci95
		Weighted mode	7	0.552594835	-0.143536007	-0.590880252	0.303808238	0.866289607	0.553839552	1.355009192
Intervertebral Disk Degeneration	Triacylglycerol (49:2) levels	MR Egger	7	0.584537602	-0.54906529	-2.391636515	1.293505934	0.577489343	0.091479853	3.64554522
		Weighted median	7	0.200247147	-0.177665526	-0.449535799	0.094204748	0.837222406	0.637924208	1.098784697
		Inverse variance weighted	7	0.494801408	-0.073128284	-0.283078613	0.136822046	0.929481585	0.753460554	1.146624083
		Simple mode	7	0.5874537	-0.124033975	-0.548296411	0.300228461	0.883349828	0.577933533	1.350167233
		Weighted mode	7	0.510179592	-0.135525716	-0.515031476	0.243980044	0.873256706	0.597481788	1.27631886
Intervertebral Disk Degeneration	Triacylglycerol (54:3) levels	MR Egger	7	0.466564903	0.753155579	-1.12093525	2.627246407	2.123690928	0.325974784	13.83561974
		Weighted median	7	0.8140446	-0.031118077	-0.290422732	0.228186578	0.969361107	0.74794732	1.256319706
		Inverse variance weighted	7	0.883245572	0.016505837	-0.203787579	0.236799253	1.016642811	0.815635611	1.267186708
		Simple mode	7	0.987453812	-0.002922126	-0.352340892	0.346496639	0.997082139	0.70304042	1.414104741
		Weighted mode	7	0.895409862	-0.024522732	-0.375012652	0.325967189	0.975775508	0.687280583	1.385369913

SNP, single nucleotide polymorphism; b, beta; OR, odds ratio; ci, confidence interval.

The leave-one-out test also indicated the reliability of the results (Supplementary Figures S1–S3).

Discussion

This research explored the causality between liposomes, metabolites, and the risk of IVDD through MR analysis. We identified 13 liposomes (diacylglycerol (18:1_18:3) levels, phosphatidylcholine (14:0_16:0) levels, triacylglycerol (48:2) levels, etc.) and 79 metabolites (α-hydroxyisocaproic acid levels, butyrylpropionic acid levels, N-methyltaurine levels, etc.) might be linked to IVDD risk. Mediation analyses showed that triacylglycerol (48:2) levels could influence IVDD risk through three metabolites (3-methylcytidine levels, IMP to phosphate ratio, ADP to glycine ratio).

IVD is an avascular soft tissue structure situated in the intervertebral space. It is made up of the cartilaginous endplate, AF, and NP. IVDD, one of the most prevalent health issues worldwide, is considered to be a critical factor contributing to back and neck problems (36). Reduced levels of HDL and increased levels of TGs and LDL are the hallmarks of dyslipidemia. Lipid metabolism displays critical physiological functions in our body. Disorders of lipid metabolism can lead to obesity, hyperlipidemia, and hypercholesterolemia (37). A large-scale early cohort study involving 928 participants in the Wakayama Spine Study has revealed a possible link between disorders of lipid metabolism and IVDD (5). Zhang et al. found that clinically, age, BMI, and serum TGs were increased in the IVDD group by comparing IVDD grades with obesity-related elements in 128 volunteers and even once age and BMI are taken into account, TGs remain a significant risk factor for IVDD (38). Moreover, cell culture studies revealed that hypertriglyceridemia mediates disc cell apoptosis and matrix catabolism mainly through the MAPK signaling pathway, especially the ERK pathway (38). One of the risk factors for atherosclerosis is elevated blood TC. The four pairs of lumbar arteries and the central sacral artery are among the branch arteries of the abdominal aorta that may become blocked by atherosclerosis, which supplies blood to the lumbar spine. This obstruction further affects the blood supply to the IVD (39). Kauppila et al. found that advanced atherosclerotic manifestations of the aorta, particularly narrowing of the segmental arterial foramina above and below the IVDs, were associated with elevated IVDD grades, as assessed by routine autopsy of 86 lumbosacral spinal plain films and the corresponding abdominal aorta (39). The segmental arterioles' stenosis was associated with elevated IVDD grades (40). High TGs play an essential function in IVDD development. Nevertheless, the underlying mechanisms still need to be completed. It is exciting that the present MR analysis identified three possible intermediary factors between TGs and IVDD.

IMP is a purine nucleotide essential to living organisms and enables animals to perceive fresh flavors (41–43). Zhang et al. found that oral administration of IMP to mice promoted the exogenous fatty acid uptake and conversion to TGs and enhanced the phosphorylation of liver IMP-activated protein kinase, resulting in adipose tissue hyperplasia (44). Obesity and being overweight are

10.3389/fendo.2024.1403523

A

exposure	outcome	nsnp	method	pval	OR(95% CI)
Triacylglycerol (48:2) levels	3−methylcytidine levels	23	MR Egger	0.759	0.974 (0.825 to 1.150)
		23	Weighted median	0.397	0.956 (0.860 to 1.062)
		23	Inverse variance weighted	**0.010**	0.911 (0.848 to 0.978)
		23	Simple mode	0.950	0.994 (0.836 to 1.183)
		23	Weighted mode	0.888	0.987 (0.826 to 1.179)
3−methylcytidine levels	Intervertebral disk degeneration	19	MR Egger	**0.012**	1.067 (1.020 to 1.116)
		19	Weighted median	**0.029**	1.042 (1.004 to 1.082)
		19	Inverse variance weighted	**0.029**	1.042 (1.004 to 1.081)
		19	Simple mode	0.464	0.960 (0.864 to 1.068)
		19	Weighted mode	**0.038**	1.041 (1.005 to 1.079)
Triacylglycerol (48:2) levels	Intervertebral disk degeneration	24	MR Egger	0.106	1.128 (0.981 to 1.297)
		24	Weighted median	**0.040**	1.088 (1.004 to 1.180)
		24	Inverse variance weighted	**0.006**	1.083 (1.023 to 1.147)
		24	Simple mode	0.398	1.064 (0.924 to 1.226)
		24	Weighted mode	0.239	1.079 (0.954 to 1.222)

B

exposure	outcome	nsnp	method	pval	OR(95% CI)
Triacylglycerol (48:2) levels	Inosine 5′−monophosphate (IMP) to phosphate ratio	23	MR Egger	0.460	0.910 (0.713 to 1.163)
		23	Weighted median	0.347	0.930 (0.800 to 1.082)
		23	Inverse variance weighted	**0.012**	0.877 (0.791 to 0.972)
		23	Simple mode	0.543	0.912 (0.680 to 1.222)
		23	Weighted mode	0.743	0.961 (0.761 to 1.214)
Inosine 5′−monophosphate (IMP) to phosphate ratio	Intervertebral disk degeneration	20	MR Egger	0.169	1.100 (0.966 to 1.252)
		20	Weighted median	**0.002**	1.122 (1.044 to 1.206)
		20	Inverse variance weighted	**0.001**	1.089 (1.034 to 1.147)
		20	Simple mode	0.052	1.156 (1.008 to 1.326)
		20	Weighted mode	**0.042**	1.158 (1.015 to 1.321)
Triacylglycerol (48:2) levels	Intervertebral disk degeneration	24	MR Egger	0.106	1.128 (0.981 to 1.297)
		24	Weighted median	**0.040**	1.088 (1.004 to 1.180)
		24	Inverse variance weighted	**0.006**	1.083 (1.023 to 1.147)
		24	Simple mode	0.398	1.064 (0.924 to 1.226)
		24	Weighted mode	0.239	1.079 (0.954 to 1.222)

C

exposure	outcome	nsnp	method	pval	OR(95% CI)
Triacylglycerol (48:2) levels	Adenosine 5′−diphosphate (ADP) to glycine ratio	23	MR Egger	0.458	0.912 (0.719 to 1.157)
		23	Weighted median	0.250	0.923 (0.806 to 1.058)
		23	Inverse variance weighted	**0.041**	0.899 (0.812 to 0.995)
		23	Simple mode	0.667	0.951 (0.760 to 1.190)
		23	Weighted mode	0.547	0.941 (0.773 to 1.145)
Adenosine 5′−diphosphate (ADP) to glycine ratio	Intervertebral disk degeneration	26	MR Egger	0.270	0.952 (0.873 to 1.037)
		26	Weighted median	0.061	0.946 (0.893 to 1.002)
		26	Inverse variance weighted	**0.013**	0.948 (0.908 to 0.989)
		26	Simple mode	0.227	0.939 (0.850 to 1.037)
		26	Weighted mode	0.088	0.944 (0.887 to 1.006)
Triacylglycerol (48:2) levels	Intervertebral disk degeneration	24	MR Egger	0.106	1.128 (0.981 to 1.297)
		24	Weighted median	**0.040**	1.088 (1.004 to 1.180)
		24	Inverse variance weighted	**0.006**	1.083 (1.023 to 1.147)
		24	Simple mode	0.398	1.064 (0.924 to 1.226)
		24	Weighted mode	0.239	1.079 (0.954 to 1.222)

FIGURE 2
Forest plots illustrating the mediation analysis. **(A)** Triacylglycerol (48:2) levels impact on IVDD is mediated through 3-methylcytidine levels. **(B)** Triacylglycerol (48:2) levels impact on IVDD is mediated through inosine 5′-monophosphate (IMP) to phosphate ratio. **(C)** Triacylglycerol (48:2) levels impact on IVDD is mediated through adenosine 5′-diphosphate (ADP) to glycine ratio.

risk factors for lumbar radiculopathy and sciatica in both men and women, with a dose-response relationship, according to a meta-analysis that included data from 26 clinical investigations (45). Likewise, comparable findings were obtained by a recent meta-analysis that included ten cohort studies (46). This is consistent with our results. The results of the present mediated MR analysis suggest that TG levels cause a decrease in the IMP to phosphate ratio, which may be related to the negative feedback regulation caused by IMP facilitating the uptake and conversion of exogenous fatty acids to TGs.

ADP is an important signaling molecule that mediates various responses in cardiovascular, nervous, and other systems. Besides normal physiological processes, purinergic signaling facilitates numerous pathophysiological procedures, ranging from cell multiplication, polarization, cell motility, apoptosis, necrosis, vessel reshaping, and acute and chronic inflammation (47). Inflammation is strongly associated with the formation of thrombi, and platelets are vital mediators. ATP and ADP signaling have a crucial function in platelet activation. ADP triggers platelet aggregation via activation of P2Y1 and P2Y12 (48). Platelet activation and aggregation facilitate the attenuation of vascular rupture and bleeding in localized inflammatory areas, alleviating the ischemic and hypoxic conditions of tissues. Extracellular adenosine is also known as a "safety signal," which inhibits the hypoxia-induced inflammatory response in ischemia and reperfusion (49). The conversion of extracellular ATP to adenosine is core to attenuating aseptic inflammation during ischemia/reperfusion injury. Experimental studies have shown that increasing the ATP catabolism to adenosine effectively attenuates tissue damage and aseptic inflammation in ischemia and reperfusion (50, 51).

Furthermore, some experimental studies have demonstrated the protective effects of adenosine signaling in ischemia and reperfusion models, e.g., adenosine or its analogs decrease the releasing of harmful oxidative metabolites from neutrophils after occupying specific receptors on neutrophils (52). Grenz et al. performed

10.3389/fendo.2024.1403523

TABLE 4 The result of heterogeneity and horizontal pleiotropic test of liposomes on intervertebral disk degeneration.

Exposure	Outcome	Heterogeneity test				Horizontal pleiotropic test		
		Method	Q	Q_df	Q_pval	egger_intercept	SE	p-value
Sterol ester (27:1/22:6) levels	Intervertebral disk degeneration	MR Egger	13.89077819	21	0.874244879	-0.001887375	0.009168416	0.838885853
		Inverse variance weighted	13.93315494	22	0.903834646			
Diacylglycerol (18:1_18:3) levels	Intervertebral disk degeneration	MR Egger	19.00932533	20	0.521219939	0.0074244	0.010373165	0.482430598
		Inverse variance weighted	19.52159682	21	0.551717965			
Phosphatidylcholine (14:0_16:0) levels	Intervertebral disk degeneration	MR Egger	16.44131439	17	0.492793193	-0.022163533	0.010804365	0.055969753
		Inverse variance weighted	20.64935046	18	0.297471342			
Phosphatidylcholine (16:0_18:3) levels	Intervertebral disk degeneration	MR Egger	23.70408013	21	0.307616485	0.013187297	0.00922477	0.167554406
		Inverse variance weighted	26.01085003	22	0.251216472			
Phosphatidylcholine (16:0_20:4) levels	Intervertebral disk degeneration	MR Egger	10.45134115	22	0.98173024	0.001790591	0.0054553	0.745841599
		Inverse variance weighted	10.55907582	23	0.987252964			
Phosphatidylcholine (O-16:0_20:3) levels	Intervertebral disk degeneration	MR Egger	6.128808613	14	0.963139607	-0.020330983	0.009122196	0.042731161
		Inverse variance weighted	11.09608043	15	0.745754117			
Sphingomyelin (d36:2) levels	Intervertebral disk degeneration	MR Egger	23.96836866	22	0.348889671	-0.006100061	0.009386935	0.52252004
		Inverse variance weighted	24.42845199	23	0.38041063			
Sphingomyelin (d38:2) levels	Intervertebral disk degeneration	MR Egger	38.53365869	29	0.110920823	-0.000703016	0.008410177	0.933955877
		Inverse variance weighted	38.54294328	30	0.136301808			
Sphingomyelin (d42:2) levels	Intervertebral disk degeneration	MR Egger	46.43768482	36	0.114116701	-0.006188593	0.00603024	0.311615738
		Inverse variance weighted	47.79625709	37	0.11006855			
Triacylglycerol (48:2) levels	Intervertebral disk degeneration	MR Egger	23.62189526	22	0.367356244	-0.00579535	0.009329717	0.540870407
		Inverse variance weighted	24.03619477	23	0.401806434			

(Continued)

10.3389/fendo.2024.1403523

TABLE 4 Continued

Exposure	Outcome	Heterogeneity test				Horizontal pleiotropic test		
		Method	Q	Q_df	Q_pval	egger_intercept	SE	p-value
Triacylglycerol (49:1) levels	Intervertebral disk degeneration	MR Egger	28.53886612	23	0.196087888	0.004648415	0.009905815	0.643300952
		Inverse variance weighted	28.81210226	24	0.227282638			
Triacylglycerol (49:2) levels	Intervertebral disk degeneration	MR Egger	13.1641753	15	0.589618702	0.013799066	0.010238945	0.197757538
		Inverse variance weighted	14.98048125	16	0.526068579			
Triacylglycerol (54:3) levels	Intervertebral disk degeneration	MR Egger	22.47005984	28	0.759078983	0.010511095	0.007351105	0.163819813
		Inverse variance weighted	24.5145764	29	0.703173206			

SE, standard error; df, degrees of freedom.

TABLE 5 The result of heterogeneity and horizontal pleiotropic test of intervertebral disk degeneration on liposomes.

Exposure	Outcome	Heterogeneity test				Horizontal pleiotropic test		
		Method	Q	Q_df	Q_pval	egger_intercept	SE	p-value
Intervertebral disk degeneration	Sterol ester (27:1/22:6) levels	MR Egger	9.950754905	5	0.07664267	-0.024211947	0.080886725	0.776730161
		Inverse variance weighted	10.12907117	6	0.119320733			
Intervertebral disk degeneration	Diacylglycerol (18:1_18:3) levels	MR Egger	1.219625282	5	0.942980785	0.008027362	0.059936251	0.898680519
		Inverse variance weighted	1.237562972	6	0.974988725			
Intervertebral disk degeneration	Phosphatidylcholine (14:0_16:0) levels	MR Egger	3.192639974	5	0.670314185	0.006777759	0.065507709	0.921615696
		Inverse variance weighted	3.203344991	6	0.782926181			
Intervertebral disk degeneration	Phosphatidylcholine (16:0_18:3) levels	MR Egger	3.777167475	5	0.581923327	0.007269991	0.057349975	0.904066159
		Inverse variance weighted	3.793236933	6	0.704633188			
Intervertebral disk degeneration	Phosphatidylcholine (16:0_20:4) levels	MR Egger	3.64001985	5	0.602314682	0.049832406	0.057117781	0.422873204
		Inverse variance weighted	4.401188796	6	0.62255437			
Intervertebral disk degeneration	Phosphatidylcholine (O-16:0_20:3) levels	MR Egger	5.18517898	5	0.393701438	-0.086297392	0.060531778	0.213293655

(Continued)

10.3389/fendo.2024.1403523

TABLE 5 Continued

Exposure	Outcome	Heterogeneity test				Horizontal pleiotropic test		
		Method	Q	Q_df	Q_pval	egger_intercept	SE	p-value
		Inverse variance weighted	7.292944164	6	0.294603443			
Intervertebral disk degeneration	Sphingomyelin (d36:2) levels	MR Egger	1.998047208	5	0.849415176	-0.042556438	0.057309584	0.491132851
		Inverse variance weighted	2.549458954	6	0.862891874			
Intervertebral disk degeneration	Sphingomyelin (d38:2) levels	MR Egger	7.374425976	5	0.194249446	-0.062591836	0.06964914	0.410013475
		Inverse variance weighted	8.565563991	6	0.199524505			
Intervertebral disk degeneration	Sphingomyelin (d42:2) levels	MR Egger	6.056462806	5	0.300763556	-0.120285626	0.06302179	0.114586655
		Inverse variance weighted	10.4690678	6	0.106238189			
Intervertebral disk degeneration	Triacylglycerol (48:2) levels	MR Egger	5.081601017	5	0.406002948	-0.018211279	0.058235846	0.767118836
		Inverse variance weighted	5.180988268	6	0.520818582			
Intervertebral disk degeneration	Triacylglycerol (49:1) levels	MR Egger	10.80620879	5	0.055360595	-0.001033773	0.093261663	0.991584589
		Inverse variance weighted	10.80647434	6	0.094544912			
Intervertebral disk degeneration	Triacylglycerol (49:2) levels	MR Egger	6.414942119	5	0.26791002	0.036051582	0.070681085	0.6317203
		Inverse variance weighted	6.748725717	6	0.344711329			
Intervertebral disk degeneration	Triacylglycerol (54:3) levels	MR Egger	7.857534253	5	0.164263946	-0.055798919	0.071888929	0.472740603
		Inverse variance weighted	8.80430279	6	0.184886754			

SE, standard error; df, degrees of freedom.

repetitive and nontraumatic occlusion of renal arteries in each adenosine receptor gene-targeted mouse. Then, Renal vascular A2B adenosine receptors protect the kidney against ischemia, as shown by measurements of certain parameters of renal function (53). The branches of the lumbar arteries, which begin at the base of the abdominal aorta, sustain the corpus lumborum. Nevertheless, arterial sclerosis usually occurs first in the lowest branches, leading to stenosis or occlusion of the lumbar artery segments (54, 55). As a result, some inflammation and damage caused by ischemia occurs. However, whether ADP can play a protective role against vertebral ischemic injury needs to be verified by more in-depth studies.

From a molecular biology perspective, the relationship between TG and IVDD can be explored at several levels. First, certain genes associated with TG metabolism may show aberrant expression in patients with IVDD, and such changes may affect disc cell metabolism and function by affecting TG synthesis or catabolism. For example, lipoprotein lipase and lipoprotein lipase-related protein play key roles in TG metabolism (56, 57), and their

10.3389/fendo.2024.1403523

TABLE 6 The result of heterogeneity and horizontal pleiotropic test of 3 mediated relationships.

Exposure	Outcome	Heterogeneity test				Horizontal pleiotropic test		
		method	Q	Q_df	Q_pval	egger_intercept	se	pval
Triacylglycerol (48:2) levels	3-methylcytidine levels	MR Egger	20.78798429	21	0.471955826	-0.009663691	0.011039915	0.391290569
		Inverse variance weighted	21.55420628	22	0.486750455			
3-methylcytidine levels	Intervertebral disk degeneration	MR Egger	25.11094167	17	0.092253799	-0.011124871	0.00665853	0.11307325
		Inverse variance weighted	29.23426484	18	0.045590109			
Triacylglycerol (48:2) levels	Intervertebral disk degeneration	MR Egger	23.62189526	22	0.367356244	-0.00579535	0.009329717	0.540870407
		Inverse variance weighted	24.03619477	23	0.401806434			
Triacylglycerol (48:2) levels	Inosine 5'-monophosphate (IMP) to phosphate ratio	MR Egger	22.98822365	21	0.344606628	-0.005399542	0.016242271	0.742854387
		Inverse variance weighted	23.10920167	22	0.395585397			
Inosine 5'-monophosphate (IMP) to phosphate ratio	Intervertebral disk degeneration	MR Egger	8.276801264	18	0.974224776	-0.001598475	0.009806616	0.872334745
		Inverse variance weighted	8.303370154	19	0.983349345			
Triacylglycerol (48:2) levels	Intervertebral disk degeneration	MR Egger	23.62189526	22	0.367356244	-0.00579535	0.009329717	0.540870407
		Inverse variance weighted	24.03619477	23	0.401806434			
Triacylglycerol (48:2) levels	Adenosine 5'-diphosphate (ADP) to glycine ratio	MR Egger	16.4029829	21	0.74659883	-0.002064712	0.015775505	0.897115267
		Inverse variance weighted	16.42011271	22	0.794502667			
Adenosine 5'-diphosphate (ADP) to glycine ratio	Intervertebral disk degeneration	MR Egger	31.42489672	24	0.141905562	-0.000912331	0.008534701	0.915759523
		Inverse variance weighted	31.43985876	25	0.174864771			
Triacylglycerol (48:2) levels	Intervertebral disk degeneration	MR Egger	23.62189526	22	0.367356244	-0.00579535	0.009329717	0.540870407
		Inverse variance weighted	24.03619477	23	0.401806434			

SE, standard error; df, degrees of freedom.

reduced expression in patients with IVDD may lead to TG accumulation, which affects intracellular lipid homeostasis and, consequently, disc health. Second, signaling pathways related to TG metabolism may be altered in IVDD, affecting cell proliferation, differentiation, and apoptosis. For example, the insulin signaling pathway plays an important role in regulating lipid metabolism and glucose metabolism, and its abnormalities may affect energy metabolism and anabolism of intervertebral disc cells, leading to degenerative changes (58). In addition, high TG levels may trigger cellular stress responses, such as endoplasmic reticulum stress,

which affect disc cell function (59). Endoplasmic reticulum stress leads to the unfolded protein response, which activates the expression of a variety of stress-related genes and affects the balance of protein synthesis and degradation in cells, and prolonged endoplasmic reticulum stress may lead to cellular dysfunction and degeneration (60). TG accumulation may also trigger an inflammatory response, which may further exacerbate IVDD development. TG and its metabolites may affect the development of IVDD through the activation of inflammation-related signaling pathways, such as the NF-κB pathway, promoting the release of inflammatory factors, triggering an inflammatory response in the disc tissue, and further damaging the structure and function of the disc (61). Abnormal TG metabolism may also affect the synthesis and degradation of the disc's extracellular matrix, leading to degenerative changes in the intervertebral disc. For example, matrix metalloproteinases (MMPs) play an important role in degenerative disc disease (62), and abnormal TG metabolism may affect the activity of MMPs, leading to degradation of the disc matrix and affecting disc stability and elasticity (63). Oxidative stress is also a key factor in the relationship between TG and IVDD. High TG levels may trigger oxidative stress (64), leading to damage and degenerative changes in intervertebral disc cells. Oxidative stress disrupts the intracellular antioxidant balance, leading to lipid peroxidation, protein oxidation, and DNA damage, which can further affect disc cell function and disc integrity (65, 66). Finally, genes associated with metabolic syndrome may play a role in IVDD, and these genes may affect both TG metabolism and disc health. For example, PPARγ (peroxisome proliferator-activated receptor γ) plays a key role in lipid metabolism and inflammatory responses, and aberrant expression of PPARγ may affect both TG metabolism and inflammatory responses in the intervertebral discs, which may contribute to the development of IVDD (67–69). By exploring the above molecular biological mechanisms, we can gain a deeper understanding of the relationship between TG and IVDD and provide a theoretical basis for future therapeutic strategies.

Study strengths and limitations

This analysis has two strengths. First, it is the first study to investigate the relationship between liposomes and metabolites and the risk of IVDD using large-scale GWAS data, which eliminates confounders and reverse causality. This is highly beneficial in obtaining a thorough understanding of the relationship between liposomes and metabolites and the IVDD risk. Secondly, the bias was reduced through employing a two-sample study design, which involved using separate datasets for exposures and outcomes data, ensuring no intersection between the two sets of data. Nevertheless, there are certain aspects of this research that could be enhanced. Initially, the bulk of the data for this study was sourced from publicly accessible online databases; however, due to variations in platforms and geographic areas, some data might exhibit heterogeneity and may not entirely substitute for traditional research methods. Secondly, the IVDD data utilized in this study lacked specific details about the study subject, preventing a subgroup analysis based on various regions or gender. Consequently, the study outcomes might be limited in their applicability to populations from certain regions or specific genders. Finally, this study focused on analyzing causality from a genetic perspective, and the precise underlying mechanisms need to be explored in the future through necessary laboratory tests.

Conclusion

Our comprehensive MR analysis identified 13 liposomes and 79 metabolites, which may have possible causal links to IVDD. Additionally, we discovered three intermediary associations between liposomes and IVDD. These metabolites and liposomes will be useful for IVDD mechanistic research as well as clinical diagnostics for prognosis and risk assessment.

Data availability statement

The original contributions presented in the study are included in the article/Supplementary Material. Further inquiries can be directed to the corresponding authors.

Author contributions

D-QC: Conceptualization, Writing – original draft. Z-QQ: Validation, Writing – original draft. W-BX: Data curation, Software, Writing – original draft. K-YX: Formal analysis, Writing – original draft. N-KS: Visualization, Writing – original draft. H-YS: Formal analysis, Writing – original draft. J-YF: Formal analysis, Writing – original draft. G-XL: Funding acquisition, Supervision, Writing – review & editing. GR: Funding acquisition, Supervision, Writing – review & editing.

Funding

The author(s) declare financial support was received for the research, authorship, and/or publication of this article. This study received financial support from the Natural Science Foundation of Fujian Province (Grant Number: 2021J05282), Xiamen Municipal Bureau of Science and Technology (Grant Number: 3502Z20224033) and Xiamen Science and Technology Program (No. 3502Z20224ZD1003).

Acknowledgments

We express gratitude to the GWAS catalog and FinnGen database for providing relevant genetic data.

Conflict of interest

The authors declare that the research was conducted in the absence of any commercial or financial relationships that could be construed as a potential conflict of interest.

Publisher's note

All claims expressed in this article are solely those of the authors and do not necessarily represent those of their affiliated organizations, or those of the publisher, the editors and the reviewers. Any product that may be evaluated in this article, or claim that may be made by its manufacturer, is not guaranteed or endorsed by the publisher.

Supplementary material

The Supplementary Material for this article can be found online at: https://www.frontiersin.org/articles/10.3389/fendo.2024.1403523/full#supplementary-material

References

1. Yi J, Zhou Q, Huang J, Niu S, Ji G, Zheng T. Lipid metabolism disorder promotes the development of intervertebral disc degeneration. *BioMed Pharmacother*. (2023) 166:115401. doi: 10.1016/j.biopha.2023.115401

2. Raj PP. Intervertebral disc: anatomy-physiology-pathophysiology-treatment. *Pain Pract*. (2008) 8:18–44. doi: 10.1111/j.1533-2500.2007.00171.x

3. Zhang W, Sun T, Li Y, Yang M, Zhao Y, Liu J, et al. Application of stem cells in the repair of intervertebral disc degeneration. *Stem Cell Res Ther*. (2022) 13:70. doi: 10.1186/s13287-022-02745-y

4. Mohd Isa IL, Mokhtar SA, Abbah SA, Fauzi MB, Devitt A, Pandit A. Intervertebral disc degeneration: biomaterials and tissue engineering strategies toward precision medicine. *Adv Healthc Mater*. (2022) 11:e2102530. doi: 10.1002/adhm.202102530

5. Teraguchi M, Yoshimura N, Hashizume H, Muraki S, Yamada H, Oka H, et al. Metabolic syndrome components are associated with intervertebral disc degeneration: the wakayama spine study. *PloS One*. (2016) 11:e0147565. doi: 10.1371/journal.pone.0147565

6. Huang Z, Chen J, Su Y, Guo M, Chen Y, Zhu Y, et al. Impact of dyslipidemia on the severity of symptomatic lumbar spine degeneration: A retrospective clinical study. *Front Nutr*. (2022) 9:1033375. doi: 10.3389/fnut.2022.1033375

7. Zhang Y, Zhao Y, Wang M, Si M, Li J, Hou Y, et al. Serum lipid levels are positively correlated with lumbar disc herniation–a retrospective study of 790 Chinese patients. *Lipids Health Dis*. (2016) 15:80. doi: 10.1186/s12944-016-0248-x

8. Curic G. Intervertebral disc and adipokine leptin-loves me, loves me not. *Int J Mol Sci*. (2020) 22:375. doi: 10.3390/ijms22010375

9. Walsh TP, Arnold JB, Evans AM, Yaxley A, Damarell RA, Shanahan EM. The association between body fat and musculoskeletal pain: a systematic review and meta-analysis. *BMC Musculoskelet Disord*. (2018) 19:233. doi: 10.1186/s12891-018-2137-0

10. Liu C, Gao X, Lou J, Li H, Chen Y, Chen M, et al. Aberrant mechanical loading induces annulus fibrosus cells apoptosis in intervertebral disc degeneration via mechanosensitive ion channel Piezo1. *Arthritis Res Ther*. (2023) 25:117. doi: 10.1186/s13075-023-03093-9

11. Urban JP, Roberts S. Degeneration of the intervertebral disc. *Arthritis Res Ther*. (2003) 5:120–30. doi: 10.1186/ar629

12. Liuke M, Solovieva S, Lamminen A, Luoma K, Leino-Arjas P, Luukkonen R, et al. Disc degeneration of the lumbar spine in relation to overweight. *Int J Obes (Lond)*. (2005) 29:903–8. doi: 10.1038/sj.ijo.0802974

13. Francisco V, Pino J, González-Gay MÁ, Lago F, Karppinen J, Tervonen O, et al. A new immunometabolic perspective of intervertebral disc degeneration. *Nat Rev Rheumatol*. (2022) 18:47–60. doi: 10.1038/s41584-021-00713-zIF:33.7

14. Ruiz-Fernández C, Francisco V, Pino J, Mera A, González-Gay MA, Gómez R, et al. Molecular relationships among obesity, inflammation and intervertebral disc degeneration: are adipokines the common link? *Int J Mol Sci*. (2019) 20:2030. doi: 10.3390/ijms20082030

15. Hu S, Shao Z, Zhang C, Chen L, Mamun AA, Zhao N, et al. Chemerin facilitates intervertebral disc degeneration via TLR4 and CMKLR1 and activation of NF-kB signaling pathway. *Aging (Albany NY)*. (2020) 12:11732–53. doi: 10.18632/aging.103339

16. Heindel JJ, Newbold R, Schug TT. Endocrine disruptors and obesity. *Nat Rev Endocrinol*. (2015) 11:653–61. doi: 10.1038/nrendo.2015.163

17. Singla P, Bardoloi A, Parkash AA. Metabolic effects of obesity: A review. *World J Diabetes*. (2010) 1:76–88. doi: 10.4239/wjd.v1.i3.76

18. Ouchi N, Parker JL, Lugus JJ, Walsh K. Adipokines in inflammation and metabolic disease. *Nat Rev Immunol*. (2011) 11:85–97. doi: 10.1038/nri2921

19. Ottensmann L, Tabassum R, Ruotsalainen SE, Gerl MJ, Klose C, Widén E, et al. Genome-wide association analysis of plasma lipidome identifies 495 genetic associations. *Nat Commun*. (2023) 14:6934. doi: 10.1038/s41467-023-42532-8

20. NaPier Z, Kanim LEA, Arabi Y, Salehi K, Sears B, Perry M, et al. Omega-3 fatty acid supplementation reduces intervertebral disc degeneration. *Med Sci Monit*. (2019) 25:9531–7. doi: 10.12659/MSM.918649

21. Zheng J, Baird D, Borges MC, Bowden J, Hemani G, Haycock P, et al. Recent developments in mendelian randomization studies. *Curr Epidemiol Rep*. (2017) 4:330–45. doi: 10.1007/s40471-017-0128-6

22. Zhu T, Goodarzi MO. Causes and consequences of polycystic ovary syndrome: insights from mendelian randomization. *J Clin Endocrinol Metab*. (2022) 107:e899–911. doi: 10.1210/clinem/dgab757

23. Boef AG, Dekkers OM, le Cessie S. Mendelian randomization studies: a review of the approaches used and the quality of reporting. *Int J Epidemiol*. (2015) 44:496–511. doi: 10.1093/ije/dyv071

24. Lawlor DA, Harbord RM, Sterne JA, Timpson N, Davey Smith G. Mendelian randomization: using genes as instruments for making causal inferences in epidemiology. *Stat Med*. (2008) 27:1133–63. doi: 10.1002/sim.3034

25. Hartwig FP, Davies NM, Hemani G, Davey Smith G. Two-sample Mendelian randomization: avoiding the downsides of a powerful, widely applicable but potentially fallible technique. *Int J Epidemiol*. (2016) 45:1717–26. doi: 10.1093/ije/dyx028

26. Ma XY, Liu HM, Lv WQ, Qiu C, Xiao HM, Deng HW. A bi-directional Mendelian randomization study of the sarcopenia-related traits and osteoporosis. *Aging (Albany NY)*. (2022) 14:5681–98. doi: 10.18632/aging.204145

27. Chen Y, Lu T, Pettersson-Kymmer U, Stewart ID, Butler-Laporte G, Nakanishi T, et al. Genomic atlas of the plasma metabolome prioritizes metabolites implicated in human diseases. *Nat Genet*. (2023) 55:44–53. doi: 10.1038/s41588-022-01270-1

28. Burgess S, Butterworth A, Thompson SG. Mendelian randomization analysis with multiple genetic variants using summarized data. *Genet Epidemiol*. (2013) 37:658–65. doi: 10.1002/gepi.21758

29. Bowden J, Davey Smith G, Haycock PC, Burgess S. Consistent estimation in mendelian randomization with some invalid instruments using a weighted median estimator. *Genet Epidemiol*. (2016) 40:304–14. doi: 10.1002/gepi.21965

30. Bowden J, Davey Smith G, Burgess S. Mendelian randomization with invalid instruments: effect estimation and bias detection through Egger regression. *Int J Epidemiol*. (2015) 44:512–25. doi: 10.1093/ije/dyv080

31. Burgess S, Thompson SG. Interpreting findings from Mendelian randomization using the MR-Egger method. *Eur J Epidemiol*. (2017) 32:377–89. doi: 10.1007/s10654-017-0255-x

32. Niu PP, Song B, Wang X, Xu YM. Serum uric acid level and multiple sclerosis: A mendelian randomization study. *Front Genet*. (2020) 11:254. doi: 10.3389/fgene.2020.00254

33. Yavorska OO, Burgess S. MendelianRandomization: an R package for performing Mendelian randomization analyses using summarized data. *Int J Epidemiol*. (2017) 46:1734–9. doi: 10.1093/ije/dyx034

34. Yan H, Zhao S, Huang HX, Xie P, Cai XH, Qu YD, et al. Systematic Mendelian randomization study of the effect of gut microbiome and plasma metabolome on severe COVID-19. *Front Immunol*. (2023) 14:1211612. doi: 10.3389/fimmu.2023.1211612

35. Lewis RG, Simpson BGenetics, Autosomal Dominant. *StatPearls*. Treasure Island (FL: StatPearls Publishing (2023).

36. Fan C, Chu G, Yu Z, Ji Z, Kong F, Yao L, et al. The role of ferroptosis in intervertebral disc degeneration. *Front Cell Dev Biol*. (2023) 11:1219840. doi: 10.3389/fcell.2023.1219840

37. Liu HH, Li JJ. Aging and dyslipidemia: a review of potential mechanisms. *Ageing Res Rev*. (2015) 19:43–52. doi: 10.1016/j.arr.2014.12.001

38. Zhang X, Chen J, Huang B, Wang J, Shan Z, Liu J, et al. Obesity mediates apoptosis and extracellular matrix metabolic imbalances via MAPK pathway activation in intervertebral disk degeneration. *Front Physiol*. (2019) 10:1284. doi: 10.3389/fphys.2019.01284

39. Kauppila LI. Atherosclerosis and disc degeneration/low-back pain–a systematic review. *Eur J Vasc Endovasc Surg*. (2009) 37(6):661–70. doi: 10.1016/j.ejvs.2009.02.006

40. Kauppila LI, Penttilä A, Karhunen PJ, Lalu K, Hannikainen P. Lumbar disc degeneration and atherosclerosis of the abdominal aorta. *Spine (Phila Pa 1976)*. (1994) 19:923–9. doi: 10.1097/00007632-199404150-00010

41. Chaudhari N, Roper SD. Molecular and physiological evidence for glutamate (umami) taste transduction via a G protein-coupled receptor. *Ann N Y Acad Sci*. (1998) 855:398–406. doi: 10.1111/j.1749-6632.1998.tb10598.x

42. Kurihara K, Kashiwayanagi M. Physiological studies on umami taste. *J Nutr*. (2000) 30:931S–4S. doi: 10.1093/jn/130.4.931S

43. Kinnamon SC. Umami taste transduction mechanisms. *Am J Clin Nutr*. (2009) 90:753S–5S. doi: 10.3945/ajcn.2009.27462K

44. Zhang B, Xu Y, Liu J, Wu C, Zhao X, Zhou L, et al. Oral Intake of Inosine 5'-Monophosphate in Mice Promotes the Absorption of Exogenous Fatty Acids and Their Conversion into Triglycerides though Enhancing the Phosphorylation of Adenosine 5'-Monophosphate-Activated Protein Kinase in the Liver, Leading to Lipohyperplasia. *Int J Mol Sci*. (2023) 24:14588. doi: 10.3390/ijms241914588

45. Shiri R, Lallukka T, Karppinen J, Viikari-Juntura E. Obesity as a risk factor for sciatica: a meta-analysis. *Am J Epidemiol*. (2014) 179:929–37. doi: 10.1093/aje/kwu007

46. Zhang TT, Liu Z, Liu YL, Zhao JJ, Liu DW, Tian QB. Obesity as a risk factor for low back pain: A meta-analysis. *Clin Spine Surg*. (2018) 31:22–7. doi: 10.1097/BSD.0000000000000468

47. Loukovaara S, Sahanne S, Jalkanen S, Yegutkin GG. Increased intravitreal adenosine 5'-triphosphate, adenosine 5'-diphosphate and adenosine 5'-monophosphate levels in patients with proliferative diabetic retinopathy. *Acta Ophthalmol*. (2015) 93:67–73. doi: 10.1111/aos.12507

48. Eltzschig HK, Sitkovsky MV, Robson SC. Purinergic signaling during inflammation. *N Engl J Med*. (2012) 367:2322–33. doi: 10.1056/NEJMra1205750

49. Grenz A, Homann D, Eltzschig HK. Extracellular adenosine: a safety signal that dampens hypoxia-induced inflammation during ischemia. *Antioxid Redox Signal*. (2011) 15:2221–34. doi: 10.1089/ars.2010.3665

50. Hart ML, Gorzolla IC, Schittenhelm J, Robson SC, Eltzschig HK. SP1-dependent induction of CD39 facilitates hepatic ischemic preconditioning. *J Immunol*. (2010) 184:4017–24. doi: 10.4049/jimmunol.0901851

51. Grenz A, Zhang H, Hermes M, Eckle T, Klingel K, Huang DY, et al. Contribution of E-NTPDase1 (CD39) to renal protection from ischemia-reperfusion injury. *FASEB J*. (2007) 21:2863–73. doi: 10.1096/fj.06-7947com

52. Cronstein BN, Daguma L, Nichols D, Hutchison AJ, Williams M. The adenosine/neutrophil paradox resolved: human neutrophils possess both A1 and A2 receptors that promote chemotaxis and inhibit O2 generation, respectively. *J Clin Invest*. (1990) 85:1150–7. doi: 10.1172/JCI114547

53. Grenz A, Osswald H, Eckle T, Yang D, Zhang H, Tran ZV, et al. The reno-vascular A2B adenosine receptor protects the kidney from ischemia. *PloS Med*. (2008) 5:e137. doi: 10.1371/journal.0050137

54. Kauppila LI, McAlindon T, Evans S, Wilson PW, Kiel D, Felson DT. Disc degeneration/back pain and calcification of the abdominal aorta. A 25-year follow-up study in Framingham. *Spine (Phila Pa 1976)*. (1997) 22:1642–7. doi: 10.1097/00007632-199707150-00023

55. Kauppila LI. Prevalence of stenotic changes in arteries supplying the lumbar spine. *A postmortem angiographic study 140 subjects Ann Rheum Dis*. (1997) 56:591–5. doi: 10.1136/ard.56.10.591

56. Mead JR, Irvine SA, Ramji DP. Lipoprotein lipase: structure, function, regulation, and role in disease. *J Mol Med (Berl)*. (2002) 80:753–69. doi: 10.1007/s00109-002-0384-9

57. Beisiegel U, Weber W, Ihrke G, Herz J, Stanley KK. The LDL-receptor-related protein, LRP, is an apolipoprotein E-binding protein. *Nature*. (1989) 341:162–4. doi: 10.1038/341162a0

58. Akhtar A, Sah SP. Insulin signaling pathway and related molecules: Role in neurodegeneration and Alzheimer's disease. *Neurochem Int*. (2020) 135:104707. doi: 10.1016/j.neuint.2020.104707

59. Mollica MP, Lionetti L, Putti R, Cavaliere G, Gaita M, Barletta A. From chronic overfeeding to hepatic injury: role of endoplasmic reticulum stress and inflammation. *Nutr Metab Cardiovasc Dis*. (2011) 21:222–30. doi: 10.1016/j.numecd.2010.10.012

60. Chen X, Shi C, He M, Xiong S, Xia X. Endoplasmic reticulum stress: molecular mechanism and therapeutic targets. *Signal Transduct Target Ther*. (2023) 8:352. doi: 10.1038/s41392-023-01570-w

61. Lu Y, Qie D, Yang F, Wu J. LncRNA MEG3 aggravates adipocyte inflammation and insulin resistance by targeting IGF2BP2 to activate TLR4/NF-κB signaling pathway. *Int Immunopharmacol*. (2023) 121:110467. doi: 10.1016/j.intimp.2023.110467

62. Glaeser JD, Salehi K, Kanim LEA, NaPier Z, Kropf MA, Cuéllar JM, et al. NF-κB inhibitor, NEMO-binding domain peptide attenuates intervertebral disc degeneration. *Spine J*. (2020) 20:1480–91. doi: 10.1016/j.spinee.2020.04.025

63. Kozakova M, Morizzo C, Goncalves I, Natali A, Nilsson J, Palombo C. Cardiovascular organ damage in type 2 diabetes mellitus: the role of lipids and inflammation. *Cardiovasc Diabetol*. (2019) 18:61. doi: 10.1186/s12933-019-0865-6

64. Li T, Guo W, Zhou Z. Adipose triglyceride lipase in hepatic physiology and pathophysiology. *Biomolecules*. (2021) 12:57. doi: 10.3390/biom12010057

65. Wang Y, Cheng H, Wang T, Zhang K, Zhang Y, Kang X. Oxidative stress in intervertebral disc degeneration: Molecular mechanisms, pathogenesis and treatment. *Cell Prolif*. (2023) 56:e13448. doi: 10.1111/cpr.13448

66. Yang RZ, Xu WN, Zheng HL, Zheng XF, Li B, Jiang LS, et al. Involvement of oxidative stress-induced annulus fibrosus cell and nucleus pulposus cell ferroptosis in intervertebral disc degeneration pathogenesis. *J Cell Physiol*. (2021) 236(4):2725–39. doi: 10.1002/jcp.30039

67. Cheng P, Wei HZ, Chen HW, Wang ZQ, Mao P, Zhang HH. DNMT3a-mediated methylation of PPARγ promote intervertebral disc degeneration by regulating the NF-κB pathway. *J Cell Mol Med*. (2024) 28:e18048. doi: 10.1111/jcmm.18048

68. Liu Y, Qu Y, Liu L, Zhao H, Ma H, Si M, et al. PPAR-γ agonist pioglitazone protects against IL-17 induced intervertebral disc inflammation and degeneration via suppression of NF-κB signaling pathway. *Int Immunopharmacol*. (2019) 72:138–47. doi: 10.1016/j.intimp.2019.04.012

69. Sivasami P, Elkins C, Diaz-Saldana PP, Goss K, Peng A, Hamersky M4, et al. Obesity-induced dysregulation of skin-resident PPARγ+ Treg cells promotes IL-17A-mediated psoriatic inflammation. *Immunity*. (2023) 56:1844–61. doi: 10.1016/j.immuni.2023.06.021